RNA polymerase-mediated regulation of intrinsic antibiotic resistance and bacterial cell division

Vijay Soni[1*], Junhao Zhu[2,3], Yesha Patel[4], John D. Helmann[4], Eric J. Rubin[3], Kyu Y. Rhee[1*]

[1] Division of Infectious Diseases, Weill Department of Medicine, Weill Cornell Medicine NY, NY 10021
[2] CAS Key Laboratory of Pathogen Microbiology and Immunology, Institute of Microbiology, Chinese Academy of Sciences, Beijing, China
[3] Department of Immunology and Infectious Diseases, Harvard T.H. Chan School of Public Health, Boston, MA, 02115, USA
[4] Department of Microbiology, Cornell University Ithaca, NY 14853

***To whom correspondence may be addressed:** kyr9001@med.cornell.edu, vis2032@med.cornell.edu

ORCID:
Vijay Soni: https://orcid.org/0000-0002-3395-7429
Junhao Zhu: https://orcid.org/0000-0002-3301-5677
Yesha Patel: https://orcid.org/0000-0001-9888-9888
John D. Helmann: https://orcid.org/0000-0002-3832-3249
Eric J. Rubin: https://orcid.org/0000-0001-5120-962X
Kyu Y. Rhee: https://orcid.org/0000-0003-4582-2895

Keywords: RNA polymerase, Transcription, Division, Peptidoglycan, Cell wall biosynthesis, Rifampicin, MtrAB Regulon, WalKR regulon, Metabolomics, Transcriptomics, Rifampicin Resistance, Antimicrobial Resistance, Antibiotics, Two-Component Regulatory System, β-Lactams.

Abbreviations: Tuberculosis (TB), *Mycobacterium tuberculosis* (Mtb), Multi-drug resistance-(MDR), Extensive-drug resistance (XDR), Total-drug resistance (TDR), RNA Polymerase (RNAP), Rifampin (RIF), Rifampin-sensitive (rifS), Rifampin-resistant (rifR), UDP-GlcNAc (UG), Peptidoglycan (PG), Tricarboxylic acid (TCA)

ASBTRACT

Rifampin is a frontline antibiotic that inhibits the RNA polymerase of Mycobacterium tuberculosis (Mtb), the causative agent of tuberculosis (TB). Unlike most antibiotics, rifampin has an unusual ability to shorten the duration of treatment needed to cure TB that is not simply explained by its antimicrobial potency. We sought specific secondary effects of rifampin's inhibition of Mtb RNA polymerase that may mediate this activity. We discovered that rifampin elicited a cell division arrest that was mediated through its inhibition of RNA polymerase. This arrest resulted in a downstream inhibition of the MtrAB two-component regulatory system, a mediator of intrinsic antibiotic resistance in Mtb. This inhibition is broadly conserved in other bacteria and represents a novel form of antimicrobial activity, termed adjunctive sensitization, that can mediate synergy and may contribute to rifampin's unusual treatment shortening activity.

INTRODUCTION

Rifampin (RIF) is an essential component of all current frontline treatments for TB, the leading cause of deaths not only due to an infectious but also curable, disease(*1*). This essentiality is a unique product of both its potent *in vitro* activity against *Mycobacterium tuberculosis* (Mtb)(*2*), the causative agent of TB, and its clinical ability to shorten the duration of treatment needed to achieve a durable, relapse-free cure(*3, 4*). However, resistance to rifampin, a defining feature of multi- (MDR), extensively- (XDR), and totally-drug (TDR) resistant TB, is on the rise, prompting a need for therapeutically equivalent alternatives(*1*).

Biochemical, structural, and genetic evidence has demonstrated that rifampin specifically binds the beta-subunit of bacterial RNA polymerase (RNAP) and blocks the exit tunnel of nascent transcripts to prevent their extension beyond a trinucleotide length and that this binding is required for antimicrobial activity(*5*) (Fig 1A). Knowledge of whether this antimicrobial activity is mediated or accompanied by specific secondary physiologic effects or is a non-specific consequence of inhibiting transcription initiation as a whole however remains unaddressed. Studies by Mitchison, for example, specifically showed evidence of continued incorporation of ^{3}H uridine and recoverable Mtb mRNA following prolonged exposure to bactericidal concentrations of rifampin *in vitro(6)* while phenotypic studies revealed specific synergies between rifampin and β-lactam, but not protein synthesis, antibiotics(*7*). Mutations in RNAP conferring resistance to rifampin have been similarly reported to lead to changes in cell wall structure and bacterial morphology (Table S1).

Here, we provide evidence that rifampin-mediated inhibition of RNA polymerase in Mtb elicits specific physiologic changes in cell wall metabolism and division that contribute to its antimycobacterial activity. We further show that these effects are phylogenetically conserved in other bacterial species. These results thus reveal a previously unrecognized, but evolutionarily conserved, functional interaction between transcription and cell division that expands our understanding of the antimicrobial mode-of-action of a well validated molecular target.

RESULTS

Metabolic impact of RNAP inhibition

We previously demonstrated that, despite its bulk effect on RNA synthesis, rifampin elicited a specific set of metabolic changes that included a combination of some that were shared by other antibiotics and others that were specific to rifampin(*8*). We hypothesized that those specifically associated with the antimycobacterial activity of rifampin might serve as a biochemical window into its treatment shortening activity. We therefore compared the metabolic profiles of isogenic rifampin-sensitive (rifS) and -resistant (rifR) Mtb strains during the pre-lethal phase of exposure to rifampin (Fig 1A, S1A). Pathway enrichment analysis of such activity-specific metabolites revealed a statistically significant over-representation of metabolites associated with amino acids, nucleotides, peptidoglycan (PG) biosynthesis, and the tricarboxylic acid (TCA) cycle (Fig 1B, S1B, S1C). We validated the functional association of these changes with the inhibition of RNAP by profiling the metabolic responses of rifS and rifR strains of Mtb to two additional structurally and mechanistically distinct inhibitors of its RNAP, fidaxomicin (FDX) and myxopyronin B (MYXO), at similar levels of antimycobacterial activity (Fig 1B, S1D), as well as following partial transcriptional silencing of the β (*rpoB*) and β' (*rpoC*) subunits of RNAP (Fig 1C, 1D, S2, S3). We further showed that these changes were not carbon source specific (S4A) and observed in both laboratory-adapted and clinical isolates (S4B). Metabolic tracing studies of Mtb following treatment with rifampin (S5) more specifically revealed accumulations of UDP-Glc*N*Ac, GTP, ATP, and UTP indicative of an increase in PG turnover and arrest of de novo PG biosynthesis (Fig 1E).

Transcriptomic impact of RNAP inhibition

Seeking further evidence of a specific physiologic impact of rifampin, we analyzed the transcriptomes of rifS and rifR Mtb during the same pre-lethal phase of exposure to rifampin (Fig 2A, S6A). Despite its expected bulk inhibition of de novo transcription, treatment with rifampin elicited both increases and decreases in transcript abundance (Fig 2A). We next overlaid the transcriptional response of Mtb to rifampin with that of FDX, a structurally and mechanistically distinct inhibitor of RNAP to define a biologically more specific transcriptional signature of RNAP inhibition. Using an absolute cutoff ($\log_2$ fold>1 and p_{corr} <0.05), we identified an activity-specific transcriptional signature that consisted in an accumulation of 537 and depletion of 344 transcripts (Fig 2A, S6B). Functional enrichment analysis revealed a depletion of genes associated with de novo PG biosynthesis (S6C), consistent with Mtb's observed metabolic response. Further analysis of this signature revealed an enrichment of genes encoding and belonging to the *mtrAB* regulon that was not observed in rifR strains exposed to rifampin (Fig 2B, 2C). The *mtrAB* regulon consists of a two-component sensor kinase and cognate DNA-binding response regulator that was previously shown to regulate peptidoglycan remodeling enzymes required for cell growth and division and reported to mediate both drug tolerance and intrinsic drug resistance (Fig 2D)(*9-13*). Targeted qPCR analysis of *mtrAB* and a representative subset of its regulon demonstrated that this repression was specific to RNAP-targeting antibiotics (Fig 2E, S7) and carbon source independent (S8). This repression was additionally

observed in Mtb whose replication had been slowed by hypoxia, acidic pH, or nutrient (PBS) starvation (S9).

Effect of RNAP on divisome activity

Given the foregoing data, we sought to probe the functional relationship between RNAP activity and cell wall metabolism in replicating Mtb. Prior studies reported a robust but mechanistically unexplained phenotypic synergy between rifampin and cephalosporin antibiotics against Mtb(*7*). We found that this synergy is also extended to a panel of cell wall-targeting a β-lactam antibiotics (cephradine, cefadroxil, meropenem, and faropenem) that selectively inhibit FtsI (PbpB or Rv2163c)(*14-20*), the transpeptidase required for septal peptidoglycan biosynthesis during cell division(*21, 22*), but not inhibitors of other peptidoglycan biosynthesis, including vancomycin and cycloserine (Fig 3A).

Previous work had demonstrated that MtrB, the sensor kinase, localized to the cell septum via interaction with divisome components (FtsI and FtsZ) and that this interaction was required for activation of *mtrA* and its regulon(*23, 24*). We, therefore, sought to test if the impact of rifampin on *mtrAB* regulon activity might be a downstream consequence of impaired septal Z-ring formation (Fig 3B). To do so, we first tested the effect of inhibiting Z-ring formation on rifampin susceptibility by transcriptionally silencing the expression of *ftsZ* to levels that only mildly slowed but did not arrest growth (S10). This revealed a selective sensitization to rifampin, but not isoniazid, upon *ftsZ* silencing (Fig 3C, S10). Similar effects were observed upon *mtrA* knockdown (Fig 3C, S11). We further found that treatment of Mtb with FtsI inhibitors resulted in increased levels of UDP-GlcNAc (S12).

Seeking more direct evidence of the effect of rifampin on septal Z-ring assembly, we conducted single-cell time-lapse microscopy of reporter strains that either expressed fluorescent fusions of *ftsZ* and *rpoB* and were exposed to defined pulses of rifampin (S13). Owing to resource limitations and a high degree of conservation of both FtsZ and RpoB in Mtb and *M. smegmatis* (89.61% amino acid identity/94% similarity and 99% amino acid identity/95% similarity, respectively), we conducted these experiments in *M. smegmatis(25, 26)* (S14 and S15). These studies demonstrated that rifampin selectively inhibited Z-ring formation in cells that had recently or not yet initiated cell division while allowing the remainder to complete the process of chromosomal segregation and cytokinesis (Fig 3D and E, upper panels). In contrast, treatment with isoniazid revealed no such effect on Z-ring formation (Fig 3D and E, lower panels), though both isoniazid and rifampin slowed cell elongation (Fig 3E, 3F). We further quantified the fraction of cells with clear FtsZ-mCherry2B foci at different stages of cell division and found that rifampin exposure almost completely collapsed nascent Z-ring formation within 2 hours of exposure, whereas isoniazid permitted continued Z-ring assembly (Fig. 3F).

Conservation of RNAP-MtrAB interaction

The biological centrality and evolutionary conservation of both RpoB and FtsZ across bacteria taxa further led us to wonder if the foregoing effects of RNAP inhibition might also be conserved in other bacterial species (S15). Focusing specifically on bacteria genera annotated to encode orthologs (WalKR/YycFG/VicKR) of the MtrAB two-component regulatory system (Fig 4A and

B), we characterized the molecular and phenotypic effects of rifampin against *Bacillus subtilis* (BS) and *Staphylococcus aureus* (SA). Both organisms encode orthologs of *rpoB* and *ftsZ* with greater than 55% amino acid identity and 75% similarity (S15) and MtrAB orthologs exhibiting greater than 45% identity and 66% similarity (S16) with similar roles in cell wall remodeling, division, and antibiotic resistance(*27-31*) (Table S2). Moreover, exposure to rifampin, fidaxomicin and myxopyronin B in both organisms demonstrated evidence of increased levels of UDP-Glc*N*Ac (Figure 4C, S17, S18), repression of their respective *mtrAB* orthologs (Figure 4D), and phenotypic synergy with cephalosporin and carbapenem antibiotics (Figure 4E).

DISCUSSION

Owing to the biological centrality of transcription and well-defined molecular mechanism of biochemical inhibition, studies of rifampin have historically focused on its quantitative impact on rates of transcription initiation as a whole, rather than the specific physiologic consequences of that inhibition(*5*). Our studies of both rifamycin and non-rifamycin inhibitors of RNA polymerase against rifampin-sensitive and -resistant strains now shed new light on the latter. Despite its genome-scale impact, we discovered that inhibition of transcription initiation, or genetic silencing of the β- or β' subunits of RNA polymerase, elicited physiologically specific and reversible metabolic changes that tracked with its antimycobacterial activity, and were associated with both transcriptional and phenotypic inhibition of the *mtrAB* two-component regulatory system (Fig 5). This inhibition effectively sensitizes Mtb (not completely killed by inhibition of transcription) to a number of secondary host- and drug-imposed stresses, and, in doing so, reveals a previously unrecognized form of antimicrobial impact, adjunctive sensitization, that expands the scope of rifampin's antimicrobial mode-of-action.

Among currently approved TB drugs, rifampin is distinguished by its ability to shorten the duration of treatment needed to achieve a durable, relapse-free cure(*32*), an activity not simply explained by standard measures of its *in vitro* antimycobacterial potency(*33, 34*). This activity has instead been ascribed to a combination of its ability to penetrate caseous or necrotic lesions and kill the non- or slowly replicating Mtb subpopulations therein(*35-37*). However, the mechanistic basis of this activity remains incompletely defined. That rifampin's impact on *mtrAB* was both carbon source independent and extended to non- or slowly replicating Mtb populations highlights a novel mechanistic effect of high potential therapeutic importance. Treatment shortening aside, the potential for this activity to inform the development of rational mechanism-based drug combinations warrants further study.

Translational potential notwithstanding, this work extends our understanding of the fundamental biology of RNA polymerase. Previous studies of the *mtrAB* and *walKR* systems had demonstrated its interaction with and regulation of genes involved in cell division and cell wall metabolism, many of which include enzymes involved in peptidoglycan remodeling(*10-12, 29, 38, 39*). In Mtb and other bacteria, MtrAB or WalKR activity has been shown to depend on septal localization and therefore be functionally associated with Z-ring formation and cell division(*23, 24, 38-41*). As discussed previously, mutations conferring resistance to RIF (in the RpoB subunit of RNAP) in other microbes have been reported to changes in cell wall structure(*42*), bacterial morphology(*42-45*), virulence(*46*) as well as resistance to various drugs targeting peptidoglycan

biogenesis (e.g., vancomycin and daptomycin)(*47-50*) while resistance to some β-lactams and cephalosporins has conversely been reported to be associated with mutations in the *rpoB* and *rpoC* subunits of RNAP(*7, 42, 43, 51-54*) (*55, 56*) (Table S1). Our work now extends this biology further to include an even more upstream and evolutionarily conserved role of RNA polymerase and its state of transcriptional competence as a potential checkpoint regulator of cell division.

Growing evidence has implicated a broader range of physiologic roles for RNA polymerase beyond its activity as a bulk enzymatic catalyst of RNA synthesis(*43, 51, 57*). Once focused on the primary drug-target interaction, modern drug development has expanded in scope to include studies of specific secondary or downstream consequences of the drug-target interaction. Such studies have helped increase knowledge of the mechanistic basis for drug activity, and in doing so, reveal additional new potential targets whose inhibition could mimic the activity of the drug itself and/or slow/prevent the emergence of resistance. Though less well recognized, such studies have also created a window into the normal physiologic functions of the targets they inhibit.

FIGURE LEGENDS

Figure 1: Inhibition of RNAP affects peptidoglycan metabolism of Mtb: (A) Experimental scheme used to define Mtb's pre-lethal response to RNAP inhibitors (RNAPi). The inset shows the domain structure of RNAP highlighting the binding site of different RNAPi. Rifampin (RIF) binds at the exit channel. Fidaxomicin (FDX) binds at the base of the RNAP clamp. Myxopyronin B (MYXO) binds at the switch region of RNAP. **(B)** Heatmap showing statistically significant $\log_2$ fold changes (FC) in metabolite levels following a prelethal 10x MIC exposure to RNAP inhibitors both in rifS and rifR (S450L and H445Y) strains for 24 hrs. **(C)** Schematic of CRISPRi-mediated genetic inhibition of RNAP. sgRNA targeting *rpoB*, *rpoC*, and non-targeting (negative control) were electroporated into Mtb-Erdman (rifS and rifR) and gene knockdown phenotype was screened by growing mutants with and without anhydrotetracycline (ATc). Samples were collected for metabolomic profiling. **(D)** Heatmap highlighting $\log_2$ FC of metabolites upon CRISPRi-mediated silencing of RNAP subunits (RpoB and RpoC). Partial depletion of *rpoB and rpoC* was achieved using anhydrotetracycline (ATc) for 4 days, resulting in similar metabolic signatures as observed upon RNAP inhibitor administration (S2, and S3). Lower row displays matching metabolic changes of rifS-Mtb strain after RIF treatment. All results are representative of biological triplicates and two independent experiments. **(E)** Diagrammatic illustration showing the impact of RNA polymerase inhibition on peptidoglycan precursor and ribonucleotide pools in Mtb (top panel). Impact of rifampin (10x MIC dose; 0.5 µg/ml for 24 hrs) on pool sizes of GTP, UTP, Glc*N*-1P, and UDP-Glc*N*Ac in Mtb that had been prelabeled with ^{13}C and transferred to ^{12}C upon rifampin treatment. *p*-values were calculated using non-parametric t-test (for Glc*N*-1-P and GTP) or two-way ANOVA mixed model (for UTP and UDP-Glc*N*Ac). ****$p<0.0001$, and **$p<0.01$. Error bars denote s.e.m.

Figure 2: Transcriptomic profiles of Mtb RNAP inhibition by rifampin and fidaxomycin: (A) Venn diagram showing the differentially expressed and overlapping genes (in overlay) upon exposure of 10x MIC dose of rifampin and fidaxomicin to rifS strain (Mtb-H37Rv) for 24 hrs. Cutoff: $\log_2$ fold changes >1 and < -1; p_{adj} value <0.05. **(B)** Donut graph shows the functional enrichment analysis of significant overlapping genes with known functions. Almost 27.8% of genes belong to the cell wall-related mechanism and 2.8% of total genes belong to *mtrAB* regulon (see overhang) **(C)** Heatmap displaying $\log_2$ fold changes of representative members of the *mtrAB* regulon upon inhibition of RNAP both in rifS and rifR strains. Stars show the range of p_{adj} values for the most significant differential expressions calculated using the Benjamini-Hochberg method. *p* values: **< 0.05; ***<0.0005. **(D)** Depiction of the *mtrAB* regulon and its function in bacteria. Autophosphorylation or external stimuli (unknown) activates the MtrB sensor kinase which results in the downstream phosphorylation-mediated activation of its cognate response regulator MtrA and expression of almost 62 genes participating in PG remodeling, maintenance, cell shape, elongation, division, and intrinsic antimicrobial resistance (AMR). **(E)** Real-time qPCR results showing $\log_2$ fold changes of some key genes from *mtrAB* regulon after treatment of different RNAP inhibitors and antibiotics targeting cell wall or respiration. Centroid linkage hierarchical cluster analysis was done using Gene Cluster 3.0 software. All results are representative of biological triplicates and two independent experiments.

Figure 3: Impact of RNAP inhibition on divisome assembly: (A) Heatmap showing the most synergistic area score of rifampin combined with antibiotics of differing modes of action. Most synergistic area scores and Zero Interaction Potency (ZIP) scores were measured using SynergyFinder (https://synergyfinder.fimm.fi/). Scale: less than -10: antagonistic, from -10 to 10: additive, larger than 10: synergistic. All experiments were done in biological triplicates. (Table S3). **(B)** Graphic showing the impact of localization of the divisome components FtsZ *(1)* and FtsI *(2)* on the activation of MtrBA *(3)* system and their role in peptidoglycan biosynthesis and remodeling. Numbers (1,2, and 3) show the sequence of molecular events. **(C)** Dose-response graphs showing the minimum inhibitor concentrations of rifampin (RIF) and isoniazid (INH) upon partial depletion of *ftsZ* and *mtrA* in Mtb-Erdman. Gene knockdown was achieved using anhydrotetracycline (ATc) regulated CRISPRi constructs expressing respective sgRNA. **(D-F)** Subcellular localization dynamics of FtsZ and RpoB following RIF and INH treatment. Dynamics of FtsZ and RpoB were tracked in *M. smegmatis* mc^2155 cells expressing fluorescent fusions of RpoB (rpoB-msfGFP) and FtsZ (ftsZ-mCherry2B) (S13). Bacteria were grown for 9 hrs followed by 4 hrs of drug treatment (20µg/ml RIF and 25µg/ml INH) and 2 hrs of recovery. Spatial-temporal expression dynamics of the fluorescent proteins (in yellow color) were measured using Fiji and customized Python scripts. (D) Representative microscopy images illustrating Z-ring dynamics upon RIF or INH treatment. (E) Single bacteria kymographs highlighting differences in Z-ring formation between RIF and INH treated cells. The upper left panel shows that RIF inhibits FtsZ localization, whereas the right panel reveals that RIF can also halt FtsZ recruitment even after cell division has initiated. (F) Bar charts showing the percentage of cells with detectable FtsZ foci at each time point. Scale bar: 5µm. Results represent biological triplicates across two independent experiments, except for time-lapse imaging, which represents two independent experiments with biological duplicates.

Figure 4: Phylogenetic conservation of the RNAP-cell wall-division relationship: (A) A phylogenetic tree of MtrA orthologs in different bacterial species was created using https://itol.embl.de/. **(B)** Graphic presenting the conserved two-domain structure of MtrA and its orthologs. Conserved aspartic acids on the N-terminal domain and tyrosine on the C-terminal domain are targets of the sensor kinase (MtrB or WalK or YycF), while threonine on the C-terminal domain is primarily targeted by a serine-threonine protein kinase (PknB or PrkC). **(C)** Heatmap representing $\log_2$ FC of key metabolites in *B. subtilis* and *S. aureus* upon treatment with RIF, FDX, and MYXO for 20 min (S17). Respective metabolites from rifS-Mtb treated with RIF are also presented for as reference. **(D)** Real-time qPCR estimation showing the levels of two-component systems upon RIF treatment for *B. subtilis* and *S. aureus walKR*. A significant depletion is consistent with changes in the corresponding MtrAB regulon of Mtb. **(E)** Distribution of most synergistic area score showing the extent of synergy of RIF with different antibiotics both in *B. subtilis* and *S. aureus.* Lower segment is showing the overlapping antibiotic synergy score from rifS-Mtb strain. White cells indicate an absence of corresponding antibiotics. All results are representative of biological triplicates and two independent experiments.

Figure 5: Generalized model of RNAP mediated regulation of cell wall biosynthesis and bacterial division: Under normal growth conditions, bacteria maintain a state of metabolic homeostasis that provides a continuous supply of nucleotides to sustain transcription and cell

wall biosynthesis. Perturbations of transcription (either antibiotic or genetic) result in diminished turnover of nucleotides (UTP and GTP) that may affect de novo peptidoglycan biosynthesis and septa formation. The resulting imbalance leads to septum delocalization, consequently suppressing the regulon of the bacterial two component system (MtrAB/ YycFG/ WalKR or VicKR) and disrupting cell wall biosynthesis, elongation, bacterial division, and intrinsic antimicrobial resistance.

Figure 1

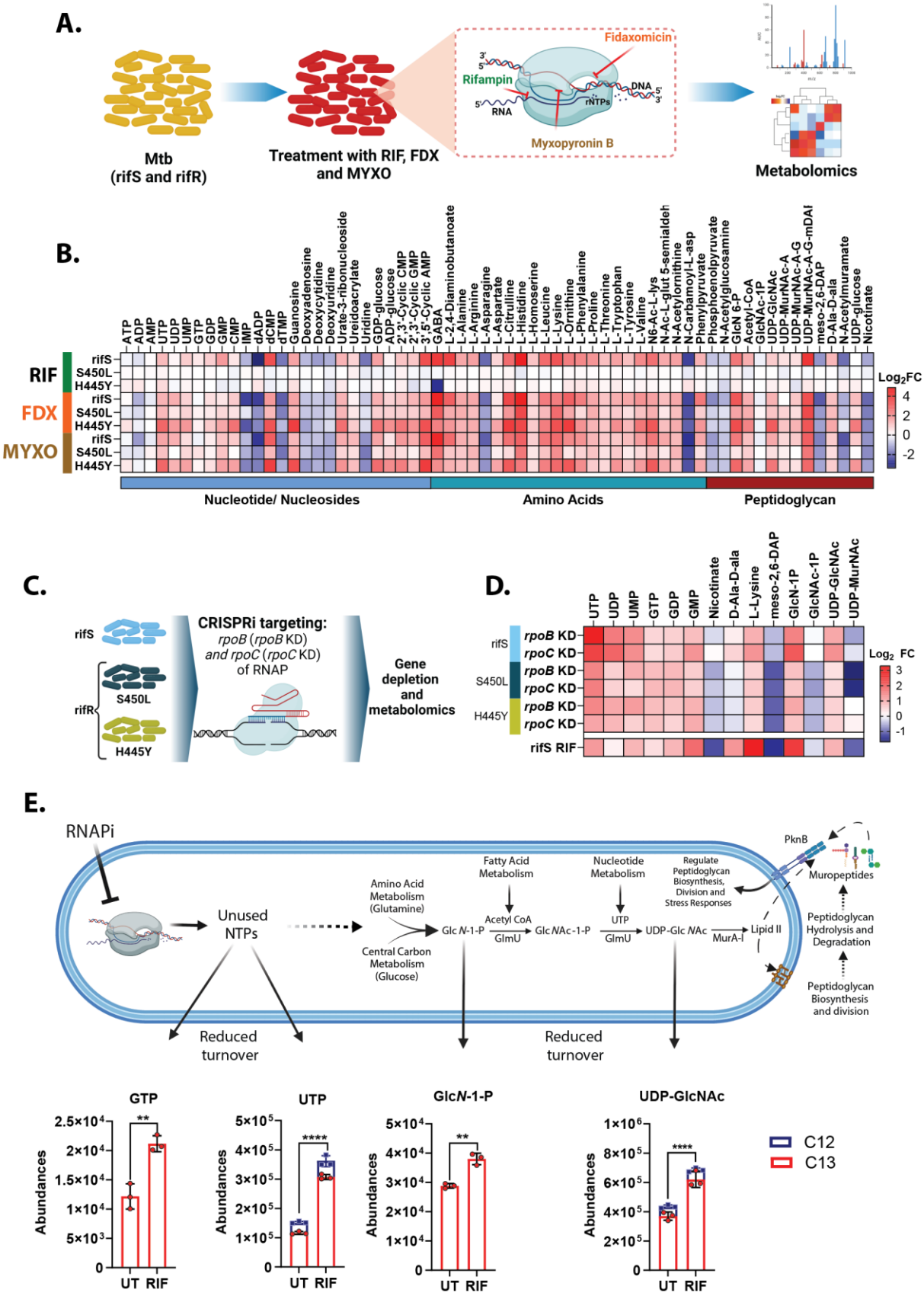
A.
Mtb
(rifS and rifR)
Treatment with RIF, FDX
and MYXO
Fidaxomicin
Rifampin
DNA
RNA
rNTPs
Myxopyronin B
Metabolomics
B.
ATP
ADP
AMP
UTP
UDP
UMP
GTP
GDP
GMP
CMP
IMP
dADP
dCMP
dTMP
Guanosine
Deoxyadenosine
Deoxycytidine
Deoxyuridine
Urate-3-ribonucleoside
Ureidoacrylate
Uridine
GDP-glucose
ADP-glucose
2',3'-Cyclic CMP
2',3'-Cyclic GMP
3',5'-Cyclic AMP
GABA
L-2,4-Diaminobutanoate
L-Alanine
L-Arginine
L-Asparagine
L-Aspartate
L-Citrulline
L-Histidine
L-Homoserine
L-Leucine
L-Lysine
L-Ornithine
L-Phenylalanine
L-Proline
L-Threonine
L-Tryptophan
L-Tyrosine
L-Valine
N6-Ac-L-lys
N-Ac-L-glut 5-semialdeh
N-Acetylornithine
N-Carbamoyl-L-asp
Phenylpyruvate
Phosphoenolpyruvate
N-Acetylglucosamine
GlcN 6-P
Acetyl-CoA
GlcNAc-1P
UDP-GlcNAc
UDP-MurNAc
UDP-MurNAc-A
UDP-MurNAc-A-G
UDP-MurNAc-A-G-mDAP
meso-2,6-DAP
D-Ala-D-ala
N-Acetylmuramate
UDP-glucose
Nicotinate
RIF
FDX
MYXO
rifS
S450L
H445Y
Log2FC
4
2
0
-2
Nucleotide/ Nucleosides
Amino Acids
Peptidoglycan
C.
rifS
rifR
S450L
H445Y
CRISPRi targeting:
rpoB (rpoB KD)
and rpoC (rpoC KD)
of RNAP
Gene
depletion
and
metabolomics
D.
UTP
UDP
UMP
GTP
GDP
GMP
Nicotinate
D-Ala-D-ala
L-Lysine
meso-2,6-DAP
GlcN-1P
GlcNAc-1P
UDP-GlcNAc
UDP-MurNAc
rifS
S450L
H445Y
rpoB KD
rpoC KD
rifS RIF
Log2 FC
3
2
1
0
-1
E.
RNAPi
Unused
NTPs
Amino Acid
Metabolism
(Glutamine)
Central Carbon
Metabolism
(Glucose)
Fatty Acid
Metabolism
Acetyl CoA
GlmU
Glc N-1-P
Glc NAc-1-P
Nucleotide
Metabolism
UTP
GlmU
UDP-Glc NAc
Regulate
Peptidoglycan
Biosynthesis,
Division and
Stress Responses
MurA-I
Lipid II
PknB
Muropeptides
Peptidoglycan
Hydrolysis and
Degradation
Peptidoglycan
Biosynthesis
and division
Reduced
turnover
Reduced
turnover
GTP
UTP
GlcN-1-P
UDP-GlcNAc
Abundances
UT
RIF
C12
C13

Figure 2

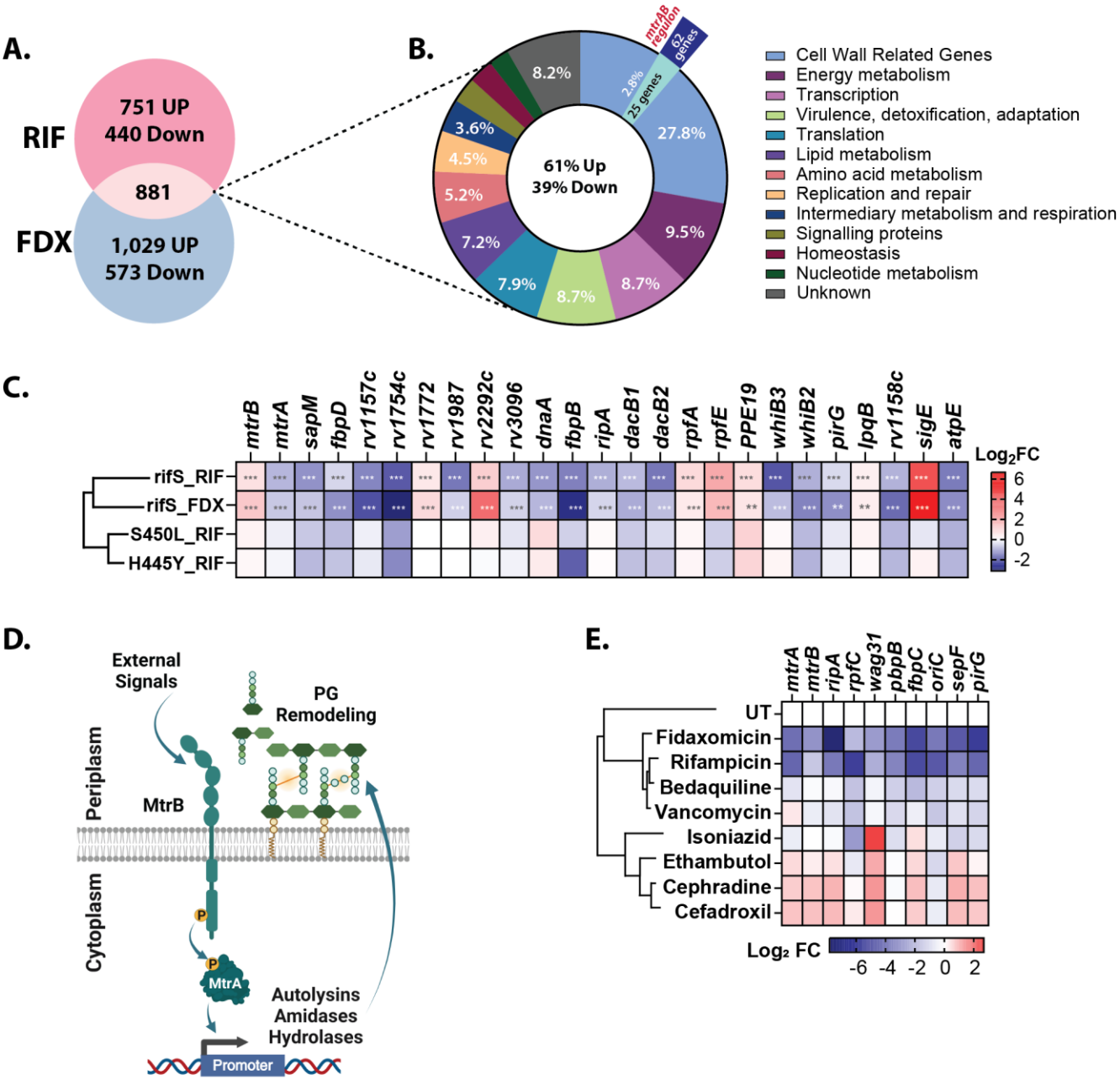
A.
RIF
751 UP
440 Down
881
FDX
1,029 UP
573 Down
B.
mtrAB regulon
62 genes
25 genes
2.8%
27.8%
9.5%
8.7%
8.7%
7.9%
7.2%
5.2%
4.5%
3.6%
8.2%
61% Up
39% Down
Cell Wall Related Genes
Energy metabolism
Transcription
Virulence, detoxification, adaptation
Translation
Lipid metabolism
Amino acid metabolism
Replication and repair
Intermediary metabolism and respiration
Signalling proteins
Homeostasis
Nucleotide metabolism
Unknown
C.
mtrB
mtrA
sapM
fbpD
rv1157c
rv1754c
rv1772
rv1987
rv2292c
rv3096
dnaA
fbpB
ripA
dacB1
dacB2
rpfA
rpfE
PPE19
whiB3
whiB2
pirG
lpqB
rv1158c
sigE
atpE
rifS_RIF
rifS_FDX
S450L_RIF
H445Y_RIF
Log2FC
6
4
2
0
-2
D.
External Signals
PG Remodeling
Periplasm
MtrB
Cytoplasm
P
MtrA
Autolysins
Amidases
Hydrolases
Promoter
E.
mtrA
mtrB
ripA
rpfC
wag31
pbpB
fbpC
oriC
sepF
pirG
UT
Fidaxomicin
Rifampicin
Bedaquiline
Vancomycin
Isoniazid
Ethambutol
Cephradine
Cefadroxil
Log2 FC
-6 -4 -2 0 2

320

Figure 3

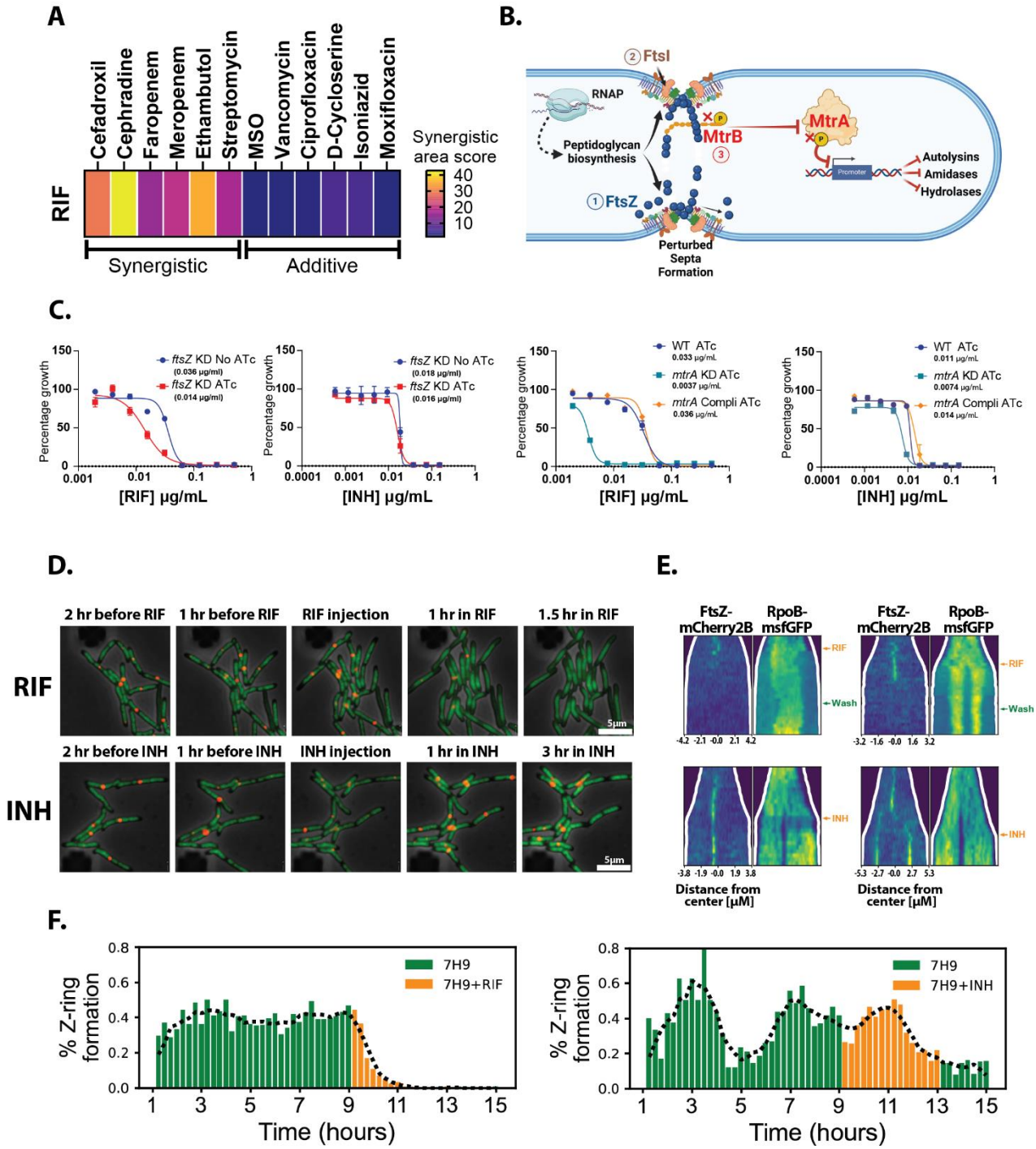
A
Cefadroxil
Cephradine
Faropenem
Meropenem
Ethambutol
Streptomycin
MSO
Vancomycin
Ciprofloxacin
D-Cycloserine
Isoniazid
Moxifloxacin
RIF
Synergistic
Additive
Synergistic area score
40
30
20
10
B.
FtsI
RNAP
Peptidoglycan biosynthesis
MtrA
MtrB
Promoter
Autolysins
Amidases
Hydrolases
FtsZ
Perturbed Septa Formation
C.
Percentage growth
ftsZ KD No ATc (0.036 µg/ml)
ftsZ KD ATc (0.014 µg/ml)
[RIF] µg/mL
ftsZ KD No ATc (0.018 µg/ml)
ftsZ KD ATc (0.016 µg/ml)
[INH] µg/mL
WT ATc 0.033 µg/mL
mtrA KD ATc 0.0037 µg/mL
mtrA Compli ATc 0.036 µg/mL
WT ATc 0.011 µg/mL
mtrA KD ATc 0.0074 µg/mL
mtrA Compli ATc 0.014 µg/mL
D.
2 hr before RIF
1 hr before RIF
RIF injection
1 hr in RIF
1.5 hr in RIF
RIF
2 hr before INH
1 hr before INH
INH injection
1 hr in INH
3 hr in INH
INH
5µm
E.
FtsZ-mCherry2B
RpoB-msfGFP
RIF
Wash
INH
Distance from center [µM]
F.
% Z-ring formation
7H9
7H9+RIF
7H9+INH
Time (hours)

321

Figure 4

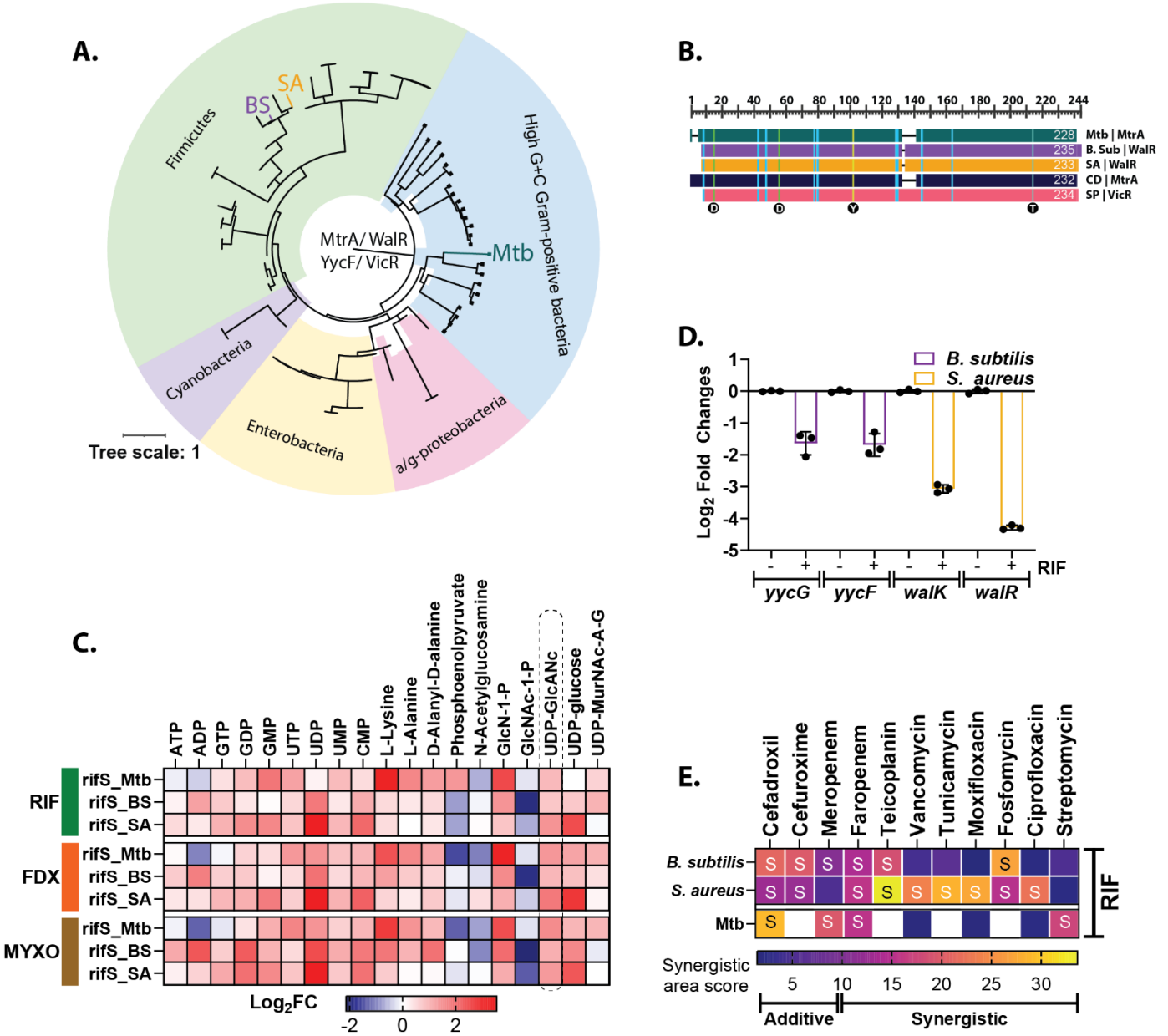
A.
Firmicutes
BS
SA
High G+C Gram-positive bacteria
MtrA/ WalR
YycF/ VicR
Mtb
Cyanobacteria
Enterobacteria
a/g-proteobacteria
Tree scale: 1
B.
1 20 40 60 80 100 120 140 160 180 200 220 244
228 Mtb | MtrA
235 B. Sub | WalR
233 SA | WalR
232 CD | MtrA
234 SP | VicR
D D Y T
C.
ATP ADP GTP GDP GMP UTP UDP UMP CMP L-Lysine L-Alanine D-Alanyl-D-alanine Phosphoenolpyruvate N-Acetylglucosamine GlcN-1-P GlcNAc-1-P UDP-GlcANc UDP-glucose UDP-MurNAc-A-G
RIF
FDX
MYXO
rifS_Mtb
rifS_BS
rifS_SA
Log2FC
-2 0 2
D.
B. subtilis
S. aureus
Log2 Fold Changes
1 0 -1 -2 -3 -4 -5
RIF
yycG yycF walK walR
E.
Cefadroxil Cefuroxime Meropenem Faropenem Teicoplanin Vancomycin Tunicamycin Moxifloxacin Fosfomycin Ciprofloxacin Streptomycin
B. subtilis
S. aureus
Mtb
RIF
Synergistic area score
5 10 15 20 25 30
Additive
Synergistic

Figure 5

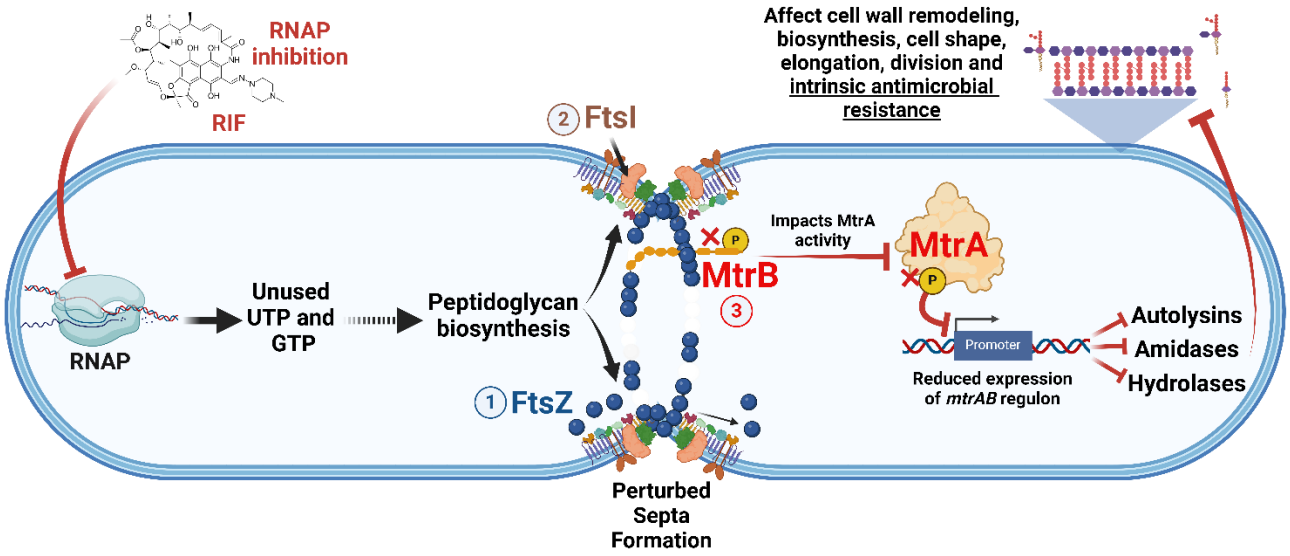
RNAP inhibition
RIF
RNAP
Unused UTP and GTP
Peptidoglycan biosynthesis
2 FtsI
1 FtsZ
3
MtrB
P
Impacts MtrA activity
MtrA
P
Promoter
Reduced expression of mtrAB regulon
Affect cell wall remodeling, biosynthesis, cell shape, elongation, division and intrinsic antimicrobial resistance
Autolysins
Amidases
Hydrolases
Perturbed Septa Formation

REFERENCES:

1. "Global tuberculosis report 2023. Geneva: World Health Organization; 2023. Licence: CC BY-NC-SA 3.0 IGO.."
2. V. Lorian, M. Finland, In vitro effect of rifampin on mycobacteria. *Appl Microbiol* **17**, 202-207 (1969).
3. W. Fox, G. A. Ellard, D. A. Mitchison, Studies on the treatment of tuberculosis undertaken by the British Medical Research Council tuberculosis units, 1946-1986, with relevant subsequent publications. *Int J Tuberc Lung Dis* **3**, S231-279 (1999).
4. D. A. Mitchison, The action of antituberculosis drugs in short-course chemotherapy. *Tubercle* **66**, 219-225 (1985).
5. E. A. Campbell *et al.*, Structural mechanism for rifampicin inhibition of bacterial rna polymerase. *Cell* **104**, 901-912 (2001).
6. J. M. Dickinson, P. S. Jackett, D. A. Mitchison, The effect of pulsed exposures to rifampin on the uptake of uridine- 14 C by Mycobacterium tuberculosis. *Am Rev Respir Dis* **105**, 519-527 (1972).
7. S. Ramon-Garcia *et al.*, Repurposing clinically approved cephalosporins for tuberculosis therapy. *Sci Rep* **6**, 34293 (2016).
8. M. Nandakumar, C. Nathan, K. Y. Rhee, Isocitrate lyase mediates broad antibiotic tolerance in Mycobacterium tuberculosis. *Nat Commun* **5**, 4306 (2014).
9. S. Li *et al.*, CRISPRi chemical genetics and comparative genomics identify genes mediating drug potency in Mycobacterium tuberculosis. *Nat Microbiol* **7**, 766-779 (2022).
10. E. J. R. Peterson *et al.*, MtrA modulates Mycobacterium tuberculosis cell division in host microenvironments to mediate intrinsic resistance and drug tolerance. *Cell Rep* **42**, 112875 (2023).
11. P. Gorla *et al.*, MtrA Response Regulator Controls Cell Division and Cell Wall Metabolism and Affects Susceptibility of Mycobacteria to the First Line Antituberculosis Drugs. *Front Microbiol* **9**, 2839 (2018).
12. A. K. Sharma *et al.*, MtrA, an essential response regulator of the MtrAB two-component system, regulates the transcription of resuscitation-promoting factor B of Mycobacterium tuberculosis. *Microbiology (Reading)* **161**, 1271-1281 (2015).
13. H. T. Nguyen, K. A. Wolff, R. H. Cartabuke, S. Ogwang, L. Nguyen, A lipoprotein modulates activity of the MtrAB two-component system to provide intrinsic multidrug resistance, cytokinetic control and cell wall homeostasis in Mycobacterium. *Mol Microbiol* **76**, 348-364 (2010).
14. G. A. Botta, J. T. Park, Evidence for involvement of penicillin-binding protein 3 in murein synthesis during septation but not during cell elongation. *J Bacteriol* **145**, 333-340 (1981).
15. C. Eberhardt, L. Kuerschner, D. S. Weiss, Probing the catalytic activity of a cell division-specific transpeptidase in vivo with beta-lactams. *J Bacteriol* **185**, 3726-3734 (2003).
16. P. J. Hedge, B. G. Spratt, Resistance to beta-lactam antibiotics by re-modelling the active site of an E. coli penicillin-binding protein. *Nature* **318**, 478-480 (1985).
17. P. Kumar *et al.*, Mycobacterium abscessus l,d-Transpeptidases Are Susceptible to Inactivation by Carbapenems and Cephalosporins but Not Penicillins. *Antimicrob Agents Chemother* **61**, (2017).
18. Z. Lu *et al.*, Structures of Mycobacterium tuberculosis Penicillin-Binding Protein 3 in Complex with Five beta-Lactam Antibiotics Reveal Mechanism of Inactivation. *Mol Pharmacol* **97**, 287-294 (2020).
19. F. Olivenca *et al.*, Uncovering Beta-Lactam Susceptibility Patterns in Clinical Isolates of Mycobacterium tuberculosis through Whole-Genome Sequencing. *Microbiol Spectr* **10**, e0067422 (2022).
20. G. G. Zhanel, A. E. Simor, L. Vercaigne, L. Mandell, G. Canadian Carbapenem Discussion, Imipenem and meropenem: Comparison of in vitro activity, pharmacokinetics, clinical trials and adverse effects. *Can J Infect Dis* **9**, 215-228 (1998).
21. P. Datta *et al.*, Interaction between FtsW and penicillin-binding protein 3 (PBP3) directs PBP3 to mid-cell, controls cell septation and mediates the formation of a trimeric complex involving FtsZ, FtsW and PBP3 in mycobacteria. *Mol Microbiol* **62**, 1655-1673 (2006).

396 22. M. S. Pavelka, Jr., S. Mahapatra, D. C. Crick, Genetics of Peptidoglycan Biosynthesis. *Microbiol Spectr* **2**,
397 MGM2-0034-2013 (2014).
398 23. R. Plocinska *et al.*, Mycobacterium tuberculosis MtrB sensor kinase interactions with FtsI and Wag31
399 proteins reveal a role for MtrB distinct from that regulating MtrA activities. *J Bacteriol* **196**, 4120-4129
400 (2014).
401 24. R. Plocinska *et al.*, Septal localization of the Mycobacterium tuberculosis MtrB sensor kinase promotes
402 MtrA regulon expression. *J Biol Chem* **287**, 23887-23899 (2012).
403 25. J. Zhu *et al.*, Spatiotemporal localization of proteins in mycobacteria. *Cell Rep* **37**, 110154 (2021).
404 26. J. H. Zhu *et al.*, Rifampicin can induce antibiotic tolerance in mycobacteria via paradoxical changes in rpoB
405 transcription. *Nat Commun* **9**, 4218 (2018).
406 27. H. Takada, H. Yoshikawa, Essentiality and function of WalK/WalR two-component system: the past,
407 present, and future of research. *Biosci Biotechnol Biochem* **82**, 741-751 (2018).
408 28. S. Dubrac, P. Bisicchia, K. M. Devine, T. Msadek, A matter of life and death: cell wall homeostasis and the
409 WalKR (YycGF) essential signal transduction pathway. *Mol Microbiol* **70**, 1307-1322 (2008).
410 29. L. K. R. Sharkey *et al.*, The two-component system WalKR provides an essential link between cell wall
411 homeostasis and DNA replication in Staphylococcus aureus. *mBio* **14**, e0226223 (2023).
412 30. G. S. Dobihal, Y. R. Brunet, J. Flores-Kim, D. Z. Rudner, Homeostatic control of cell wall hydrolysis by the
413 WalRK two-component signaling pathway in Bacillus subtilis. *Elife* **8**, (2019).
414 31. S. Dubrac, T. Msadek, Tearing down the wall: peptidoglycan metabolism and the WalK/WalR (YycG/YycF)
415 essential two-component system. *Adv Exp Med Biol* **631**, 214-228 (2008).
416 32. A. Jindani *et al.*, Four-Month High-Dose Rifampicin Regimens for Pulmonary Tuberculosis. *NEJM Evid* **2**,
417 EVIDoa2300054 (2023).
418 33. J. M. Dickinson, V. R. Aber, D. A. Mitchison, Bactericidal activity of streptomycin, isoniazid, rifampin,
419 ethambutol, and pyrazinamide alone and in combination against Mycobacterium Tuberculosis. *Am Rev*
420 *Respir Dis* **116**, 627-635 (1977).
421 34. A. Jindani, V. R. Aber, E. A. Edwards, D. A. Mitchison, The early bactericidal activity of drugs in patients with
422 pulmonary tuberculosis. *Am Rev Respir Dis* **121**, 939-949 (1980).
423 35. D. Menzies *et al.*, Four Months of Rifampin or Nine Months of Isoniazid for Latent Tuberculosis in Adults. *N*
424 *Engl J Med* **379**, 440-453 (2018).
425 36. Y. Liao *et al.*, Targeted Theranostics for Tuberculosis: A Rifampicin-Loaded Aggregation-Induced Emission
426 Carrier for Granulomas Tracking and Anti-Infection. *ACS Nano* **14**, 8046-8058 (2020).
427 37. V. A. Dartois, E. J. Rubin, Anti-tuberculosis treatment strategies and drug development: challenges and
428 priorities. *Nat Rev Microbiol* **20**, 685-701 (2022).
429 38. T. Fukushima *et al.*, A role for the essential YycG sensor histidine kinase in sensing cell division. *Mol*
430 *Microbiol* **79**, 503-522 (2011).
431 39. S. Dubrac, I. G. Boneca, O. Poupel, T. Msadek, New insights into the WalK/WalR (YycG/YycF) essential signal
432 transduction pathway reveal a major role in controlling cell wall metabolism and biofilm formation in
433 Staphylococcus aureus. *J Bacteriol* **189**, 8257-8269 (2007).
434 40. K. Fukuchi *et al.*, The essential two-component regulatory system encoded by yycF and yycG modulates
435 expression of the ftsAZ operon in Bacillus subtilis. *Microbiology (Reading)* **146 (Pt 7)**, 1573-1583 (2000).
436 41. K. J. Wayne *et al.*, Localization and cellular amounts of the WalRKJ (VicRKX) two-component regulatory
437 system proteins in serotype 2 Streptococcus pneumoniae. *J Bacteriol* **192**, 4388-4394 (2010).
438 42. V. L. Campodonico, D. Rifat, Y. M. Chuang, T. R. Ioerger, P. C. Karakousis, Altered Mycobacterium
439 tuberculosis Cell Wall Metabolism and Physiology Associated With RpoB Mutation H526D. *Front Microbiol*
440 **9**, 494 (2018).
441 43. Y. Patel, V. Soni, K. Y. Rhee, J. D. Helmann, Mutations in rpoB That Confer Rifampicin Resistance Can Alter
442 Levels of Peptidoglycan Precursors and Affect beta-Lactam Susceptibility. *mBio* **14**, e0316822 (2023).

443 44. A. D. Giddey *et al.*, Cell Wall Proteomics Reveal Phenotypic Adaption of Drug-Resistant Mycobacterium
444 smegmatis to Subinhibitory Rifampicin Exposure. *Frontiers in Medicine* **8**, (2021).
445 45. F. J. Abadi, P. E. Carter, P. Cash, T. H. Pennington, Rifampin resistance in Neisseria meningitidis due to
446 alterations in membrane permeability. *Antimicrob Agents Chemother* **40**, 646-651 (1996).
447 46. G. E. Louw *et al.*, Rifampicin reduces susceptibility to ofloxacin in rifampicin-resistant Mycobacterium
448 tuberculosis through efflux. *Am J Respir Crit Care Med* **184**, 269-276 (2011).
449 47. C. Hafer, Y. Lin, J. Kornblum, F. D. Lowy, A. C. Uhlemann, Contribution of selected gene mutations to
450 resistance in clinical isolates of vancomycin-intermediate Staphylococcus aureus. *Antimicrob Agents*
451 *Chemother* **56**, 5845-5851 (2012).
452 48. L. Cui *et al.*, An RpoB mutation confers dual heteroresistance to daptomycin and vancomycin in
453 Staphylococcus aureus. *Antimicrob Agents Chemother* **54**, 5222-5233 (2010).
454 49. M. M. Mwangi *et al.*, Tracking the in vivo evolution of multidrug resistance in Staphylococcus aureus by
455 whole-genome sequencing. *Proc Natl Acad Sci U S A* **104**, 9451-9456 (2007).
456 50. A. M. Turner *et al.*, Rifaximin prophylaxis causes resistance to the last-resort antibiotic daptomycin. *Nature*,
457 (2024).
458 51. Y. H. Lee, K. H. Nam, J. D. Helmann, A mutation of the RNA polymerase beta' subunit (rpoC) confers
459 cephalosporin resistance in Bacillus subtilis. *Antimicrob Agents Chemother* **57**, 56-65 (2013).
460 52. V. V. Panchal *et al.*, Evolving MRSA: High-level beta-lactam resistance in Staphylococcus aureus is
461 associated with RNA Polymerase alterations and fine tuning of gene expression. *PLoS Pathog* **16**, e1008672
462 (2020).
463 53. S. G. Palace *et al.*, RNA polymerase mutations cause cephalosporin resistance in clinical Neisseria
464 gonorrhoeae isolates. *Elife* **9**, (2020).
465 54. C. J. Kristich, J. L. Little, Mutations in the beta subunit of RNA polymerase alter intrinsic cephalosporin
466 resistance in Enterococci. *Antimicrob Agents Chemother* **56**, 2022-2027 (2012).
467 55. A. F. Adedeji-Olulana *et al.*, Two codependent routes lead to high-level MRSA. *Science* **386**, 573-580 (2024).
468 56. S. Watanabe *et al.*, Metabolic remodeling by RNA polymerase gene mutations is associated with reduced
469 beta-lactam susceptibility in oxacillin-susceptible MRSA. *mBio* **15**, e0033924 (2024).
470 57. A. L. Shiver *et al.*, Chemical-genetic interrogation of RNA polymerase mutants reveals structure-function
471 relationships and physiological tradeoffs. *Mol Cell* **81**, 2201-2215 e2209 (2021).
472 58. A. I. Wong, J. M. Rock, CRISPR Interference (CRISPRi) for Targeted Gene Silencing in Mycobacteria. *Methods*
473 *Mol Biol* **2314**, 343-364 (2021).
474 59. B. Yadav, K. Wennerberg, T. Aittokallio, J. Tang, Searching for Drug Synergy in Complex Dose-Response
475 Landscapes Using an Interaction Potency Model. *Comput Struct Biotechnol J* **13**, 504-513 (2015).
476 60. A. Ianevski, A. K. Giri, T. Aittokallio, SynergyFinder 3.0: an interactive analysis and consensus interpretation
477 of multi-drug synergies across multiple samples. *Nucleic Acids Res* **50**, W739-W743 (2022).
478 61. Z. Wang *et al.*, Mode-of-action profiling reveals glutamine synthetase as a collateral metabolic vulnerability
479 of M. tuberculosis to bedaquiline. *Proc Natl Acad Sci U S A* **116**, 19646-19651 (2019).
480 62. S. Ma *et al.*, Transcriptional regulator-induced phenotype screen reveals drug potentiators in
481 Mycobacterium tuberculosis. *Nat Microbiol* **6**, 44-50 (2021).
482 63. B. Langmead, S. L. Salzberg, Fast gapped-read alignment with Bowtie 2. *Nat Methods* **9**, 357-359 (2012).
483 64. S. Anders, P. T. Pyl, W. Huber, HTSeq--a Python framework to work with high-throughput sequencing data.
484 *Bioinformatics* **31**, 166-169 (2015).
485 65. M. I. Love, W. Huber, S. Anders, Moderated estimation of fold change and dispersion for RNA-seq data with
486 DESeq2. *Genome Biol* **15**, 550 (2014).
487 66. Z. Pang *et al.*, MetaboAnalyst 6.0: towards a unified platform for metabolomics data processing, analysis
488 and interpretation. *Nucleic Acids Res* **52**, W398-W406 (2024).
489 67. D. Tang *et al.*, SRplot: A free online platform for data visualization and graphing. *PLoS One* **18**, e0294236
490 (2023).

491 68. I. L. Bergval, P. R. Klatser, A. R. Schuitema, L. Oskam, R. M. Anthony, Specific mutations in the
492 Mycobacterium tuberculosis rpoB gene are associated with increased dnaE2 expression. *FEMS Microbiol*
493 *Lett* **275**, 338-343 (2007).
494 69. G. P. Bisson *et al.*, Upregulation of the phthiocerol dimycocerosate biosynthetic pathway by rifampin-
495 resistant, rpoB mutant Mycobacterium tuberculosis. *J Bacteriol* **194**, 6441-6452 (2012).
496 70. M. Xiao *et al.*, A novel point mutation in RpoB improves osmotolerance and succinic acid production in
497 Escherichia coli. *BMC Biotechnol* **17**, 10 (2017).
498 71. H. Maughan, B. Galeano, W. L. Nicholson, Novel rpoB mutations conferring rifampin resistance on Bacillus
499 subtilis: global effects on growth, competence, sporulation, and germination. *J Bacteriol* **186**, 2481-2486
500 (2004).
501 72. C. Wang *et al.*, Evolution of resistance mechanisms and biological characteristics of rifampicin-resistant
502 Staphylococcus aureus strains selected in vitro. *BMC Microbiol* **19**, 220 (2019).
503 73. M. Matsuo *et al.*, Mutation of RNA polymerase beta subunit (rpoB) promotes hVISA-to-VISA phenotypic
504 conversion of strain Mu3. *Antimicrob Agents Chemother* **55**, 4188-4195 (2011).
505 74. A. Okada *et al.*, Walkmycin B targets WalK (YycG), a histidine kinase essential for bacterial cell growth. *J*
506 *Antibiot (Tokyo)* **63**, 89-94 (2010).
507 75. A. Jansen *et al.*, Role of insertion elements and yycFG in the development of decreased susceptibility to
508 vancomycin in Staphylococcus aureus. *Int J Med Microbiol* **297**, 205-215 (2007).
509 76. H. Peng *et al.*, WalK(S221P), a naturally occurring mutation, confers vancomycin resistance in VISA strain
510 XN108. *J Antimicrob Chemother* **72**, 1006-1013 (2017).
511 77. M. Shoji *et al.*, walK and clpP mutations confer reduced vancomycin susceptibility in Staphylococcus aureus.
512 *Antimicrob Agents Chemother* **55**, 3870-3881 (2011).
513 78. S. Tan, K. Cho, J. R. Nodwell, A defect in cell wall recycling confers antibiotic resistance and sensitivity in
514 Staphylococcus aureus. *J Biol Chem* **298**, 102473 (2022).
515 79. N. N. Mishra, A. Rubio, C. C. Nast, A. S. Bayer, Differential Adaptations of Methicillin-Resistant
516 Staphylococcus aureus to Serial In Vitro Passage in Daptomycin: Evolution of Daptomycin Resistance and
517 Role of Membrane Carotenoid Content and Fluidity. *Int J Microbiol* **2012**, 683450 (2012).
518 80. Y. Song, A. Rubio, R. K. Jayaswal, J. A. Silverman, B. J. Wilkinson, Additional routes to Staphylococcus aureus
519 daptomycin resistance as revealed by comparative genome sequencing, transcriptional profiling, and
520 phenotypic studies. *PLoS One* **8**, e58469 (2013).
521 81. L. Friedman, J. D. Alder, J. A. Silverman, Genetic changes that correlate with reduced susceptibility to
522 daptomycin in Staphylococcus aureus. *Antimicrob Agents Chemother* **50**, 2137-2145 (2006).
523 82. B. P. Howden *et al.*, Evolution of multidrug resistance during Staphylococcus aureus infection involves
524 mutation of the essential two component regulator WalKR. *PLoS Pathog* **7**, e1002359 (2011).
525 83. C. A. Arias *et al.*, Genetic basis for in vivo daptomycin resistance in enterococci. *N Engl J Med* **365**, 892-900
526 (2011).
527 84. N. Moker *et al.*, Deletion of the genes encoding the MtrA-MtrB two-component system of Corynebacterium
528 glutamicum has a strong influence on cell morphology, antibiotics susceptibility and expression of genes
529 involved in osmoprotection. *Mol Microbiol* **54**, 420-438 (2004).
530 85. A. Fay *et al.*, The DnaK Chaperone System Buffers the Fitness Cost of Antibiotic Resistance Mutations in
531 Mycobacteria. *mBio* **12**, (2021).
532 86. B. Bosch *et al.*, Genome-wide gene expression tuning reveals diverse vulnerabilities of M. tuberculosis. *Cell*
533 **184**, 4579-4592 e4524 (2021).
534 87. E. Ballinger *et al.*, Opposing reactions in coenzyme A metabolism sensitize Mycobacterium tuberculosis to
535 enzyme inhibition. *Science* **363**, (2019).
536 88. M. Brauer *et al.*, Myxopyronin B inhibits growth of a Fidaxomicin-resistant Clostridioides difficile isolate and
537 interferes with toxin synthesis. *Gut Pathog* **14**, 4 (2022).

Acknowledgments: We thank to TBRU and TB-alliance for providing various RNAP inhibitors in this study. We thank Jenny Zhaoying Xiang and Adrian Y Tan from the Genomics core of Weill Cornell Medicine for their constant support for RNA sequencing and genomics analysis. We acknowledge Dirk Schnappinger, and Jeremy Rock for providing CRISPRi strains of *ftsZ* and *mtrA*. We also thank Michael DeJesus, Nicholas Poulton, Shuqi Li, Dr. Cara Boutte, Kristin Burns-Huang, Allison Fay, Daniel Fitzgerald, David Alland, David Sherman, Murty Madiraju, and Dr. Dhandayuthapani S. for their help with different clinical, lab, and drug-resistant strains. Thanks to Jennifer Herrmann from Helmholtz Institute for Pharmaceutical Research Saarland, Germany for generously providing Myxopyronin B.

Funding:

K.Y.R.: National Institutes of Health grant: U19 AI162584

K.Y.R.: Bill & Melinda Gates Foundation: BMGF INV-004709

J.D.H.: National Institutes of Health grant: R35GM122461

Author contributions:

Conceptualization: V.S. and K.Y.R.

Methodology: V.S., K.Y.R., J.Z.

Investigation: V.S. and K.Y.R.

Visualization: V.S. and K.Y.R.

Funding acquisition: K.Y.R.

Project administration: K.Y.R.

Supervision: K.Y.R.

Writing – original draft: V.S. and K.Y.R.

Writing – review & editing: V.S., K.Y.R., Y.P, J.D.H., and E.J.R.

Competing interests: The authors declare that they have no competing interests.

Data and materials availability: Raw metabolomics data are available at Metabolomics Workbench under the project ID PR002179. Additionally, the raw transcriptomics data are deposited to the NCBI Short Read Archive with the BioProject ID PRJNA1181268. All code used to generate cell kymographs and representative micrographs was deposited on GitHub and available at https://github.com/jzrolling/FtsZ_kymographs. Other data are available in the supplementary materials.

570